PROCEEDINGS, 50th Workshop on Geothermal Reservoir Engineering
Stanford University, Stanford, California, February 10-12, 2025
SGP-TR-229

Update on the Geology, Temperature, Fracturing, and Resource Potential at the Cape Geothermal Project Informed by Data Acquired from the Drilling of Additional Horizontal EGS Wells

Steven Fercho, Jack Norbeck, Sireesh Dadi, Gabe Matson, Jarret Borell, Emma McConville, Susanna Webb, Chris Bowie, Greg Rhodes

200 S Virginia St. Suite 220, Reno, NV 89501

Steve@Fervoenergy.com

Keywords: Horizontal Drilling, Fervo, Cape, FORGE, EGS

ABSTRACT

Fervo Energy has completed the drilling of additional deep horizontal geothermal enhanced geothermal system (EGS) wells at Project Cape, following the completion of the first deep geothermal wells at the Frisco pad that was reported in 2023. The new wells were drilled north of Fervo's Frisco Pad and west of the DOE's FORGE project in Milford Valley on two new pads called the Gold Pad and Bearskin Pad. New datasets collected through Fervo drilling have substantially increased knowledge of the geology, temperature, state of stress, and natural fracturing in Milford Valley, updating our 3D basin models with an unprecedented amount of well data and showing remarkably consistent geology, temperatures, and stress conditions throughout the development area. Temperature and depth to the granitic basement reservoir measured in the new northern wells have validated our pre-drill basin-scale models and demonstrate a high degree of predictability within the basin. Image logs from the wellfield confirm a consistent maximum horizontal stress orientation (SHmax) of NNE-SSW, which contrasts with a dominant natural fracture orientation of NNW-SSE. Stimulation of the first series of laterals on the Frisco pad have demonstrated consistent fracture growth with precise MEQ orientations measured in well DAS fiber and surface array seismometers. The application of EGS type curve theory using completions engineering design demonstrates that energy production and thermal decline can be effectively forecasted in horizontal well EGS systems.

1. INTRODUCTION

This paper describes advances in the geologic, thermal, and structural modeling conducted for Project Cape in the Milford Basin, Utah with datasets collected from the drilling, logging, and stimulation of numerous new wells at the project. The 3D geologic model first described in Fercho et al., 2024 has been progressively refined through ongoing drilling and logging efforts, allowing for a better understanding of Milford Basin's stratigraphy and thermal regime. This paper also discusses the unique variability of tuffaceous units encountered in the vertical well sections during drilling, which have been tracked through the field with unprecedented detail for a Basin and Range setting. A key component of Fervo's work at Project Cape is the development of a temperature model that integrates data from many wells, including those from Fervo, FORGE, Blundell, and historical exploration efforts. The temperature model, constructed using controlled 3D interpolation techniques, provides highly accurate temperature predictions across the field, which have been validated through log data from drilled wells. This paper further investigates the stress field, natural fracture orientations, and hydraulicly stimulated fractures at Cape, which indicate that hydraulic fractures are primarily activating pre-existing natural fractures, a finding that may influence the planning of future enhanced geothermal systems (EGS) in hard rock settings. By leveraging both geological and temperature data, the study offers valuable insights into the behavior of geothermal reservoirs and the optimization of drilling and stimulation strategies. Finally, this paper uses the application of well-established EGS type curve theory using modern completions engineering design parameters (e.g., lateral length, perforation cluster spacing, stimulated reservoir volume geometry, etc.) to show energy production and thermal decline can be effectively forecasted in horizontal well EGS systems.

2. UPDATE ON THE GEOLOGY AND TEMPERATURE OF CAPE

2.1 Geologic Model

To understand the subsurface and aid targeting of Fervo's wells at Project Cape, Fervo created a 3D geologic model (Fercho et al., 2024). The 3D model was informed by interpretation of lithologies from all available well logs as well as gravity profiles from a high-resolution gravity survey collected by Fervo. The initial 3D geologic model created by Fervo was used to predict the expected depths of major formations in the Frisco, Gold, and Bearskin lateral wells to estimate casing set points and drilling conditions, and ensure that the wells were targeted with low fault likelihood. Upon drilling and logging each new well, the geologic model was progressively refined and accuracy was improved.

From youngest to oldest, the overall stratigraphic framework of the Cape model consists of Miocene to present day basin-fill deposits, Quaternary to late Miocene volcanics and volcaniclastic sediments, and granitic basement comprised of Oligocene and Miocene plutons ranging in composition from granite, granodiorite, diorite, to monzonite, as well as large blocks of Precambrian gneiss (Simmons et al., 2019). The basin-fill deposits contain a distinct smectite clay layer likely caused by ancient lake deposits that were identified through Fervo drilling and mapped distally through correlation with a distinct magnetotelluric conductive zone (Fercho et al., 2024). The contact between the basin-fill and granitoid dips 25°-35° to the west (Figure 2). Quaternary faults have been mapped in the region, including the NNE-striking E-dipping Opal Mound fault which controls the Roosevelt Hot Springs hydrothermal system, and the Mineral Mountains West Fault System of N-striking fault scarps terminate in the southern portion of the field (Kirby et al., 2018) (Figure 1). No faults mapped at surface are known to contact Fervo's Cape development area, which is situated in low-permeability granitic plutons at reservoir depth.

Within the Cape development area, the granitic basement deepens from east to west, but it is relatively flat from south to north (Figure 3) since the Milford basin itself trends south-north. This basement geometry has allowed the targeting of a rack of horizontal wells along the basin that have very consistent shallow clay contacts and granitic basement contacts, allowing the standardization of well design, bit selection, and overall reduction of subsurface risk for the development (El Sadi et al., 2024). Within the south-north section, there is a very gradual deepening of the granitic basement contact by around 700 feet over a mile of horizontal distance, which is matched by a deepening of the 347°F (175°C) and 392°F (200°C) temperature contours, leading to a gradual deepening in the designed well depths as the development moves northwards.

While the granitic, >175°C reservoir formation is highly consistent and predictable across the field, the intermediate vertical portions of the wells have encountered remarkable variations in the thickness of tuffaceous units within the alluvial fill. Within the Frisco wells, two distinct and thin welded tuff units were encountered, with the first averaging 60 ft thick starting at ~2600 ft and the second deeper unit averaging 150 ft thick and starting at ~4300 ft (Figure 3). As the Bearskin pad was drilled, the shallow welded tuff was not encountered but the deeper welded tuff was at depth consistent with the Frisco wells, with a thickness of 200-500 ft thickening towards the south. With the subsequent drilling of the Gold wells a similar outcome was expected because these wells were drilled between the Frisco and Bearskin wells; however, instead a surprisingly thick (2,300 ft) interval of welded tuffs from 1900-4200 ft was encountered. Such variability of volcanics and alluvial fill in the Basin and Range is perhaps not uncommon; however, rarely have so many wells drilled on such a regular spacing to allow variability to be mapped at this level of detail (Figure 3). Since no significant faulting has been encountered at the surface or subsurface between these thickness changes, a leading theory is that the tuffs were deposited within a deep paleo-canyon or drainage during Miocene eruptive events. The present day location of the Mag Wash (Figure 1) supports the idea that there has been a drainage near this location throughout the development of the basin, and can be seen coming out of large a canyon in the Mineral Mountains and continuing through the surficial sediments as a topographic wash which opens up near the Gold wells. While the variability of tuffaceous units within the vertical portions of the Fervo wells has been recorded with an unprecedented amount of detail and is geologically notable, these tuffs have had little to no effect on the performance of the drilling program because they do not present drilling hazards and are positioned behind intermediate unperforated casing.

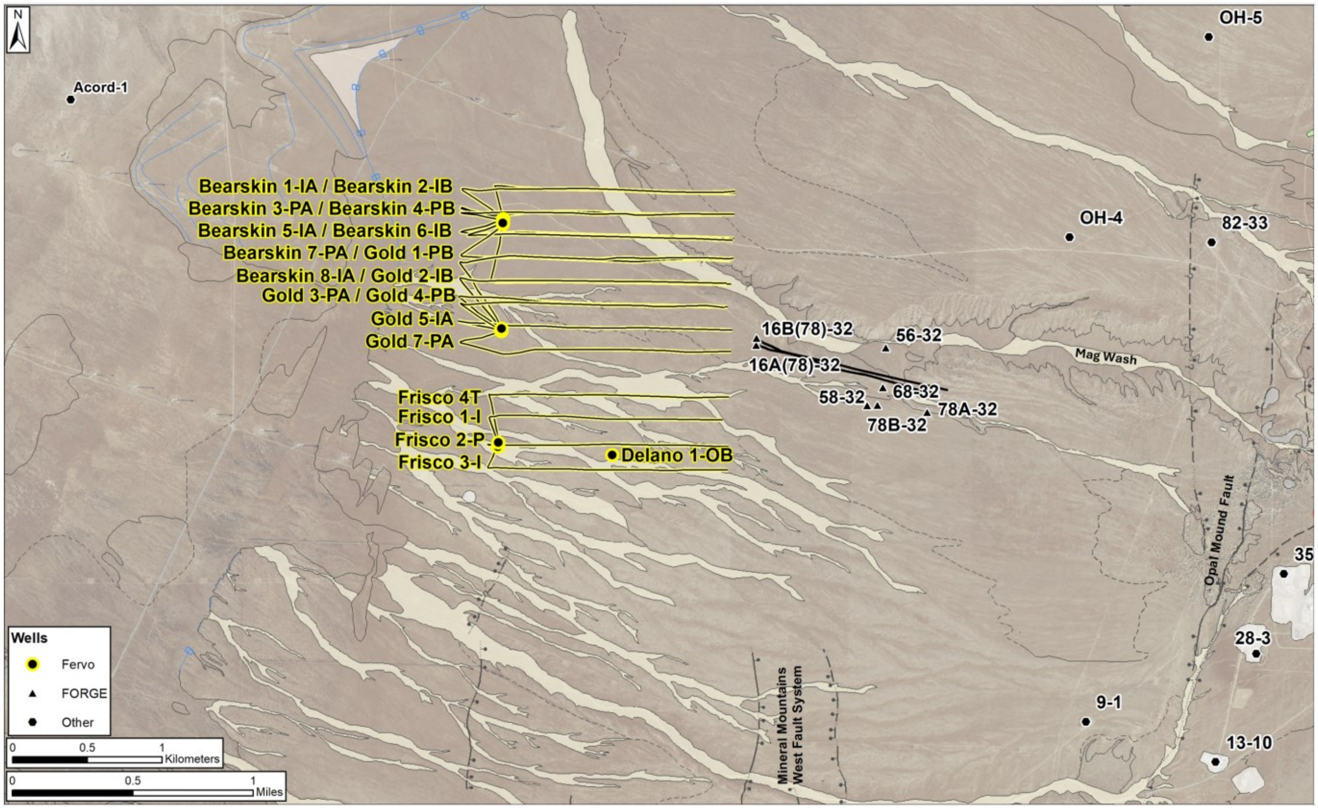

Figure 1: Map showing Fervo's completed and planned wells at the Frisco/Gold/Bearskin pads, other wells, and surface mapped faults in the Milford Valley, UT. Fault surface traces from Kirby et al. (2018).

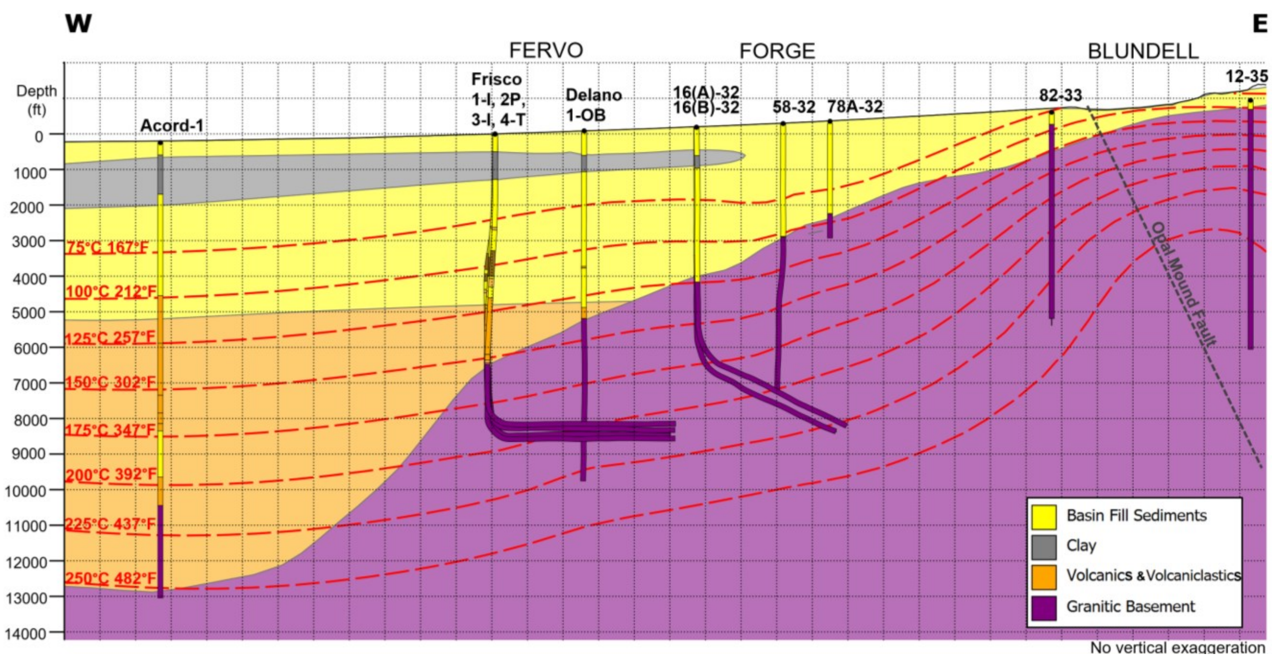

Figure 2: West-east cross section (looking north) showing the lateral wells drilled by Fervo, as wells as wells from FORGE and Blundell, shown with major formation types and measured temperatures (Fercho et al., 2024). Acord-1 lies around 1.5 miles north of section.

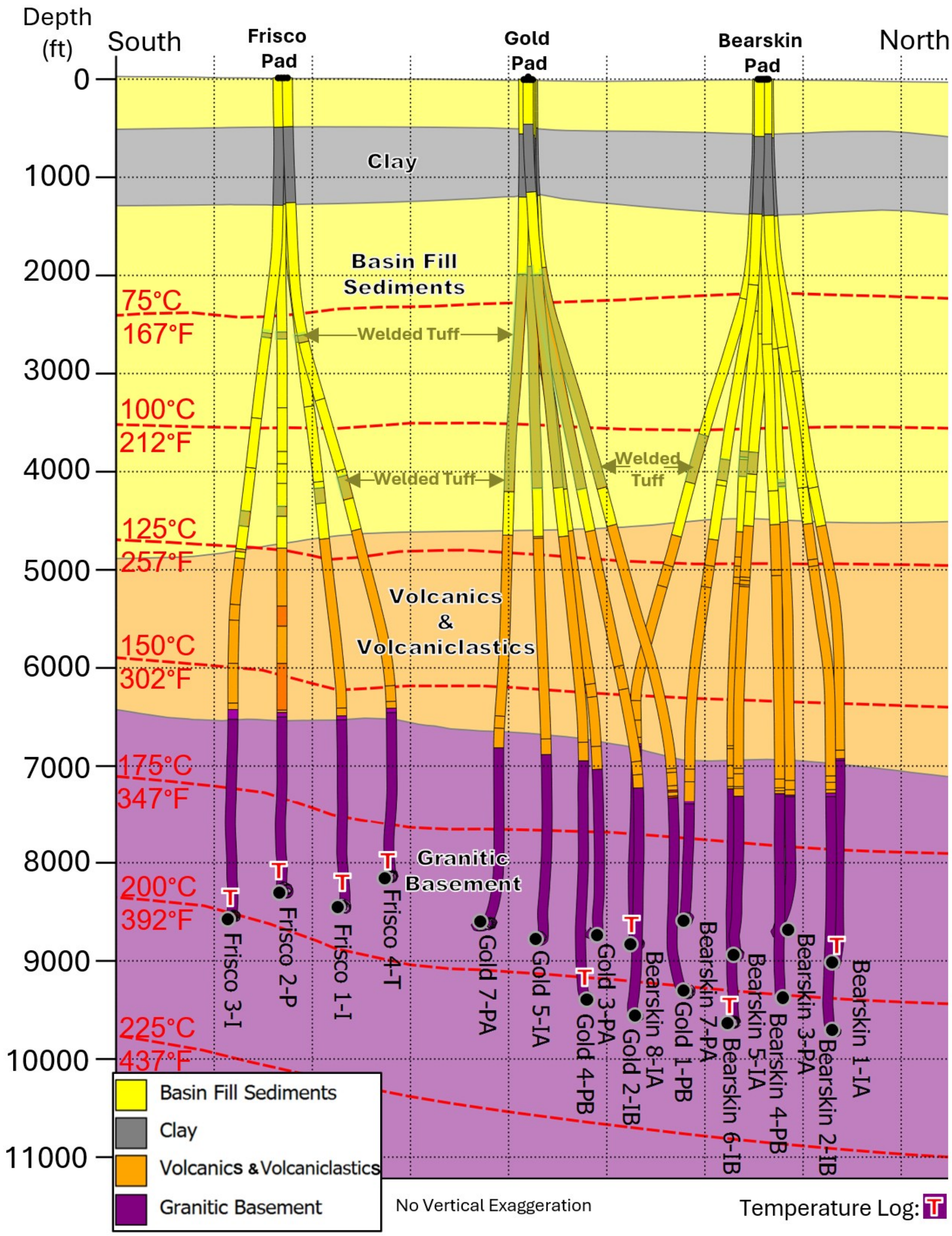

Figure 3: North-south cross section (looking west) showing the lateral wells drilled by Fervo to date, along with major formation types and measured temperatures. Wells with equilibrated temperature logs are labeled with the T symbol.

2.2 Temperature Model

The Cape 3D temperature model uses temperature data from existing Fervo, FORGE, Blundell, and historic exploration wells in the Milford basin combined with statistically derived temperature gradients in areas lacking well data (Fercho et al, 2024). 3D interpolation of the measured and statistically controlled temperature data was then completed using a Radial Basis Function (RBF) using Leapfrog Energy software. The resulting model shows that the shallowest, highest temperatures lie at the eastern edge of the basin, where the Blundell conventional hydrothermal system brings hot fluids near surface through convection within deeply connected normal faults (Figure 2). Farther west, at the FORGE and Fervo Cape wells, temperatures are lower but still elevated within the un-faulted basin due to lateral conduction from the Blundell hydrothermal system, low crustal thickness from Basin and Range extension, and thermal insulation from the 5,000-7,000 ft (1.5-2.1 km) thick cover of insulating basin-fill sediments and volcanics. At the most westward extent of the model, the historic Acord-1 well provides measured temperature control for the deepest point of the basin, anchoring 347°F (175°C) at 9055 ft (2.76 km).

After drilling out the Frisco pad, Fervo temperature logged all Frisco wells through their vertical sections and partly through the directional build curve of each well after 2-4 months of heat up. The logged temperature profiles for all four Frisco wells were very close to what was predicted by Fervo's 3D temperature model, measuring 2-10°F hotter than predicted at depth. These temperature logs were then incorporated into the temperature model, improving its accuracy (Fercho et al., 2024). Bearskin 1-IA was the first new lateral well to be drilled by Fervo after the Frisco Pad and lies approximately one mile north of the Frisco wells. Based on Frisco-updated 3D temperature model, Bearskin 1-IA was predicted to reach 369°F (187°C) at 8,500 ft. After approximately 1 month of heat-up, a temperature log was run in Bearskin 1-IA and measured 362°F (183°C) at 8500 ft, followed by a survey after 7 months of heat-up which measured 365°F (185°C) at 8,500 ft, just *4 degrees* under the model prediction (Figure 4). The Bearskin 1-IA temperature results were then iterated back into the 3D temperature model to again improve the model accuracy, which allowed for precise temperature prediction and targeting of the wells that were subsequently drilled in the mile of horizontal space between Frisco-4T and Bearskin 1-IA. Bearskin 6-IB and Bearskin 8-IA were later drilled and logged, with measured temperatures coming to within 1 degree of predictions with the latest model. Figure 3 shows the measured temperatures contoured across Fervo's current Cape wells in a south–north profile, and indicates a stable, conductive temperature regime that is nearly flat with a slight cooling trend towards the north. With such tight temperature controls at both the northern and southern ends of the field, temperature uncertainty has been nearly eliminated from Fervo's three pad (Frisco-Gold-Bearskin) development phase of Cape drilling.

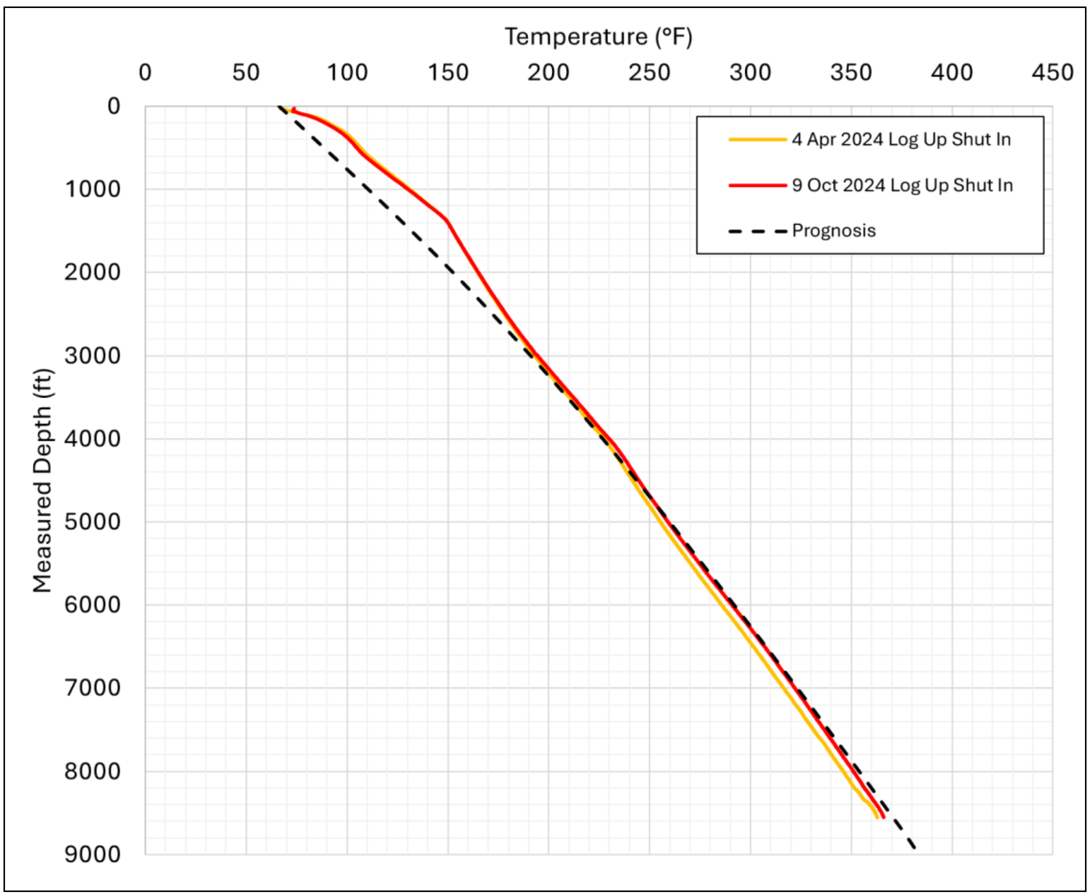

Figure 4: Predicted vs. actual temperature logs for Bearskin 1-IA

3. STRESS FIELD, NATURAL FRACTURING, AND HYDRAULICALLY INDUCED FRACTURES

Orientations of drilling induced fractures (DIFs) measured from images logs in the vertical portions of wells across Cape and FORGE areas consistently indicate and a maximum horizontal stress (SHmax) orientation of NNE (Figure 5). The DIFs measured in FORGE 58-32 and 78B-32 indicate an SHmax azimuth of ~35°, and in FORGE 16A-32 SHmax is ~15° (Simmons et al., 2019). In the Fervo Delano 1-OB image log, DIFs are tightly aligned to 10° SHmax. At the Frisco pad, image logs were collected in Frisco 1-I, 2-P, and 4-T, and DIFs measured in the vertical sections of those wells average ~15° SHmax. The combination of this Fervo DIF data with the FORGE data indicates a very consistent SHmax of NNE 10°-15° across the field, except for FORGE 58-32 and 78B-32 which have a clockwise rotation to more NE (Figure 5) which is likely more influenced by those wells' closer proximity to more complex range front-faulting.

In contrast to the *drilling induced fractures*, Figure 6 shows orientations of *natural fractures* identified from images logs across Cape and FORGE areas, colored by orientation into fracture sets. The dominant natural fracture set (Fracture Set 1) observed at Cape strikes NNW with azimuth ranging from 335°-345°, which is 25°-35° rotated counterclockwise from SHmax. The next most prominent fracture set (Fracture Set 3) is more closely aligned to SHmax with a strike of NNE, and may represent more a recent episode of fracturing. The contrast between the currently measured SHmax orientation of NNW and the dominant natural fracture set orientation of NNE may be indicative of older generations of fracturing in the basin, when the granitic blocks and/or the local stress were rotated during basin and range extension.

Prior to Fervo's planned stimulation program, it was unknown whether the orientation of the extensive pre-existing natural fracture fabric would influence the orientation of the hydraulically stimulated fractures, or if the stimulated fractures would follow the current stress field (SHmax) orientation which is the more typically expected outcome in artificial hydraulic stimulation. To track fracture growth during stimulation, microseismic events from distributed acoustic sensing (DAS) fiber data installed in Fervo and FORGE wells were acquired during the stimulation of Frisco 1-I, 2-P, and 3-I. A 3D velocity model was constructed using all available sonic logs from Utah FORGE wells and Fervo wells, including Delano 1-OB and Frisco 1-I. The velocity model additionally incorporated the top of the basement from 3D seismic and gravity data (Dadi et al., 2024). Linear trends from the microseismic clearly indicate the stimulated fractures are dominantly activating the existing NNW striking natural fracture fabric shown in (Figure 6), rather than aligning to SHmax. This finding indicates that proper understanding of the preexisting fracture networks is important to planning EGS stimulation in hard-rock settings such as the granite at Cape. Granitic rocks in setting such as this have not previously been stimulated with multi-stage hydraulic fracture at the scale, and stimulated fracture alignment to the natural fracture fabric may be the norm for these types of hard-rock formations. This provides an important dataset for comparison as more of these hard rock settings are stimulated in the future.

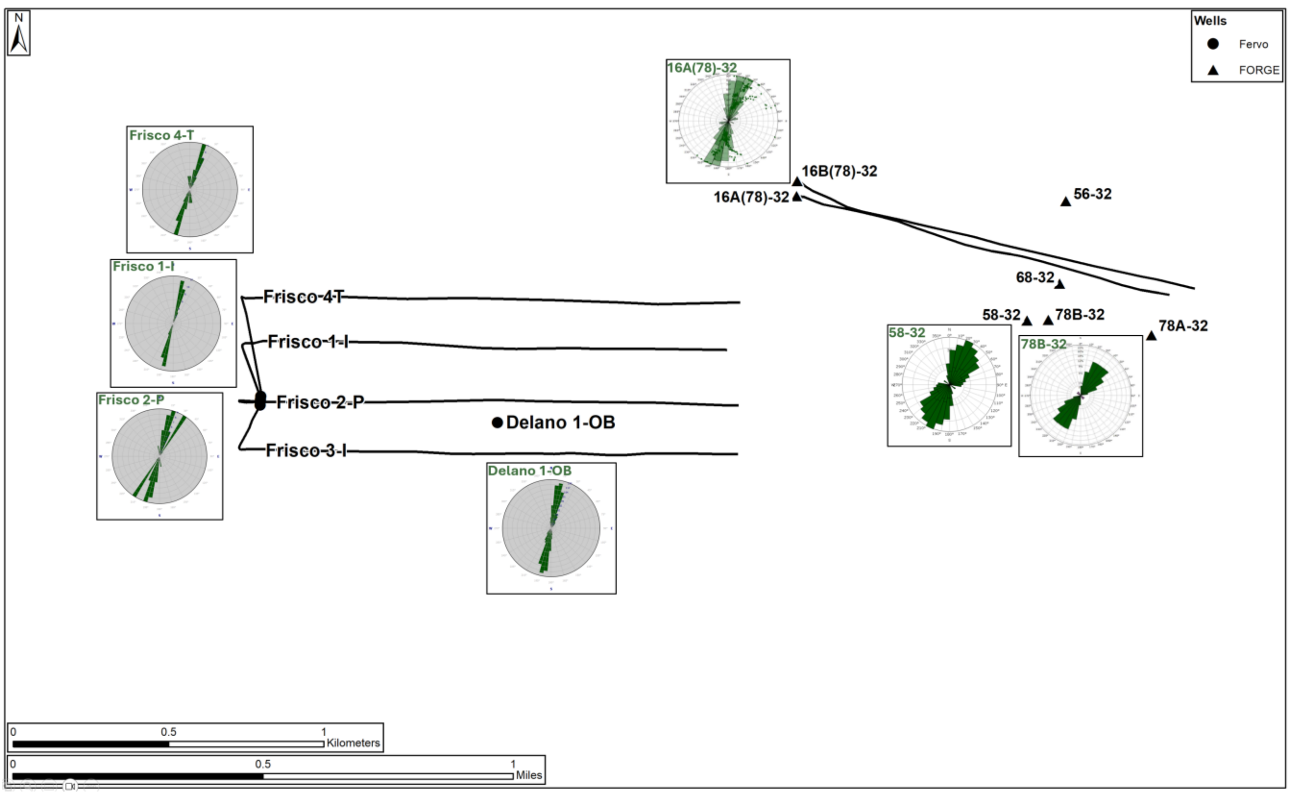

Figure 5: Orientations of drilling induced fractures (DIFs) measured from images logs in the vertical portions of wells across Cape and FORGE areas. DIFs in the Milford basin consistently indicate and SHmax orientation of NNE-SSW.

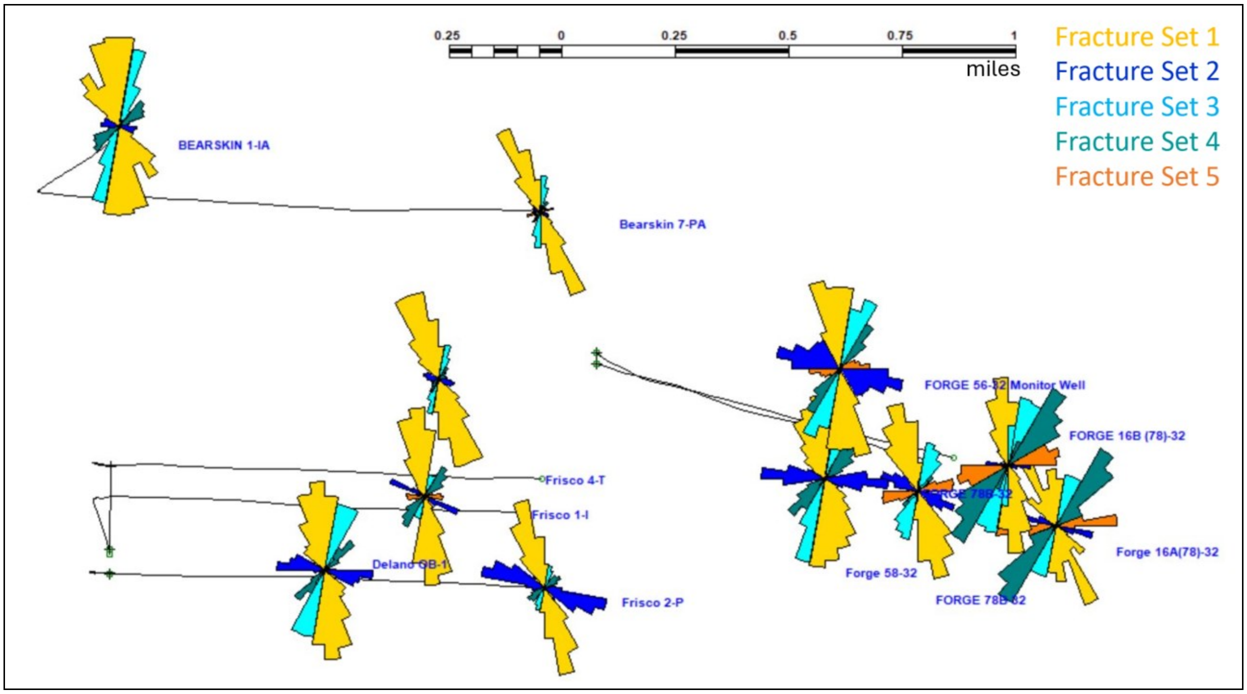

Figure 6: Orientations of natural fractures identified from images logs across Cape and FORGE areas, colored by orientation into fracture sets. The dominant natural fracture set (Fracture set 1) strikes NNW-SSE, which is 30°-50° rotated from SHmax. The next most prominent fracture set (Fracture set 3) is aligned to SHmax with a strike of NNE-SSW.

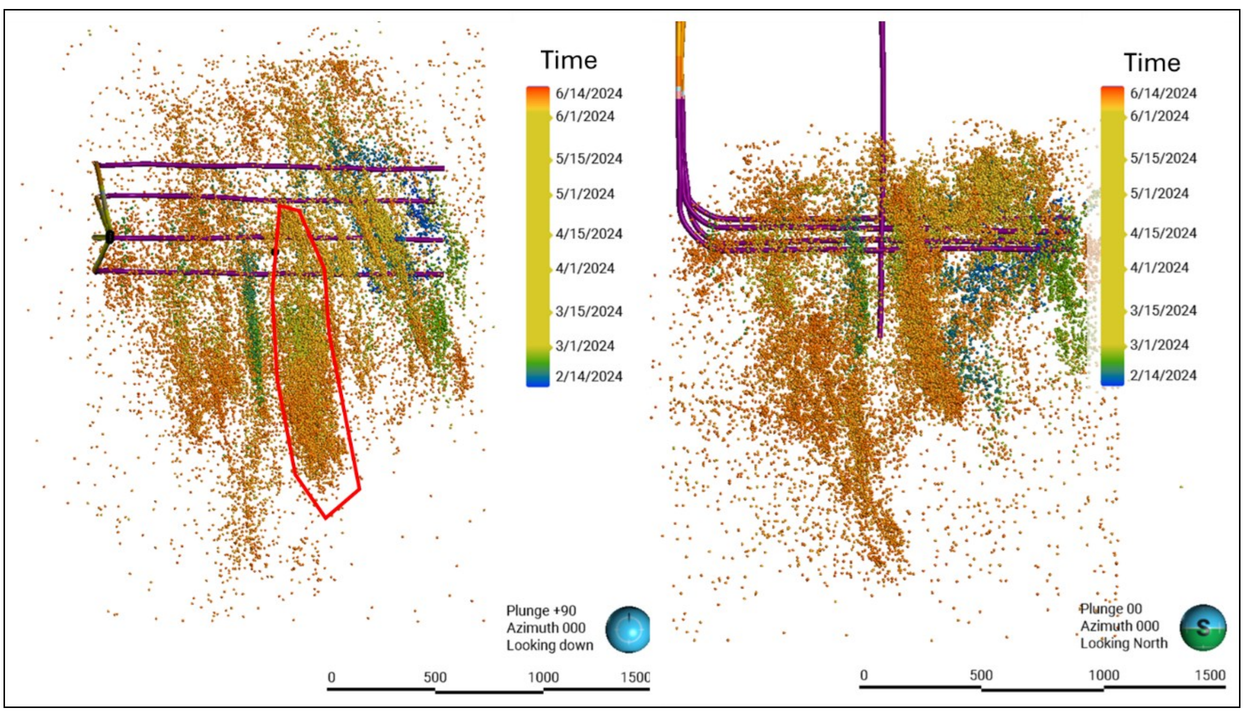

Figure 7: Microseismic cloud from DAS fiber data acquired during the stimulation of Frisco 1-I, 2-P, and 3-I (Dadi et al., 2024). Map on left and W-E section on right Linear trends from the microseismic indicate stimulated fractures are activating the existing NNW oriented natural fracture fabric shown in (Figure 6), rather than aligning to the NNE oriented SHmax. Red circle indicates an example of a NNW-oriented MEQ trend.

4. EGS TYPE CURVES

The concept for designing a geothermal system by connecting injection and production well pairs with a series of parallel fractures was first introduced in the 1970s (Gringarten et al., 1975; Brown et al., 2012). Splitting flow rates across multiple flow paths and contacting higher rock surface area for heat conduction can have a dramatic improvement in system performance. Modern horizontal drilling technology and multistage hydraulic stimulation treatment designs have recently been leveraged to validate the efficacy of this enhanced geothermal system design in several commercial-scale projects (Norbeck and Latimer, 2023; Norbeck et al., 2024). In this white paper, we outline the application of well-established EGS type curve theory using modern completions engineering design parameters (e.g., lateral length, perforation cluster spacing, stimulated reservoir volume geometry, etc.). We demonstrate that this type curve theory can be used effectively to forecast energy production and thermal decline in horizontal well EGS systems.

4.1 Gringarten Type Curves

Gringarten et al. (1975) developed geothermal type curves that can be used to predict production fluid temperature over the life of a well system. The system geometry assumed an injection well and production well that are connected by a set of evenly spaced fractures that intersect the wellbores perpendicular to the wellbore trajectory. Each of the fractures has a rectangular geometry (i.e., a fixed length and height) and a constant and uniform conductivity. The matrix rock surrounding the fractures is assumed to be impermeable, and therefore heat transfer in the matrix rock is by conduction only. As fluid flows through the fracture, heat is transferred to the fluid via the fluid-rock interface along the surface area of the fractures.

Dimensionless temperature of the produced water is defined as:

$$T_{wD} = \frac{T_{r0} - T_{wp}}{T_{r0} - T_{wi}}, \tag{1}$$

where T_{r0} is the initial reservoir temperature, T_{wp} is the produced water temperature, and T_{wi} is the injection water temperature.

Dimensionless time is defined as:

$$t_D = C_1 \left(\frac{Q}{L}\right)^2 t', \tag{2}$$

where $C_1 = (\rho_w c_w)^2 \ / \ K_r \rho_r c_r$ is a group of rock and water properties, $Q = q/(NH)$ is the volumetric flow rate (q) normalized by the number of fractures (N) and the height of the stimulated reservoir volume (H), and L is the length of the flow path between the injector and producer wells (typically taken as the offset well spacing). Time is adjusted to account for the average residence time of the water moving through the system as $t = t - L/v$, where v is the interstitial fluid velocity. For most practical problems in which we are interested in the long-term thermal behavior of the system $t \gg L/v$ and therefore $t' \approx t$.

The dimensionless fracture half-spacing is defined as:

$$x_{eD} = C_2 \left(\frac{Q}{L}\right) x_e, \tag{3}$$

where $C_2 = \rho w c w / K r$ is a different group of water and rock properties and x_e is the fracture half-spacing. For a horizontal well EGS system designed with a lateral length X_{lat} and a total of N fracture flow paths, the fracture half spacing is $x_e = X_{lat}/(2N)$. The total effective fracture surface area is then $A = NHL$. The dimensionless properties can then be redefined based on the volumetric flow rate and total fracture surface area as:

$$t_D = C_1 \left(\frac{q}{A}\right)^2 t, \tag{4}$$

and

$$x_{eD} = C_2 \left(\frac{q}{A}\right)\left(\frac{X_{lat}}{2N}\right). \tag{5}$$

$$t = \frac{1}{C_1}\left(\frac{A}{q}\right)^2 t_D, \tag{6}$$

The thermal recovery factor is defined as:

$$R = \frac{H_{pw}}{H_{r0}} = \frac{1}{2x_{eD}} \int_0^{t_D} \left[1 - T_{wD}\left(t_D\right)\right] dt_D, \tag{7}$$

or

$$R = \frac{H_{pw}}{H_{r0}} = \frac{\rho_w c_w q}{2\rho_r c_r A x_e} \int_0^{t} \left[1 - \frac{T_{r0} - T_{pw}(t)}{T_{r0} - T_{wi}}\right] dt, \tag{8}$$

The solution for T_{wD} can be obtained using the Laplace transform technique. We use a numerical inversion method to invert the Laplace transform (Cohen, 2007). Once the solution for T_{wD} is obtained, then R can be calculated using numerical integration techniques. Type curve solutions for temperature and recovery factor over time for various values of x_{eD} are shown in Figure 8 and Figure 9.

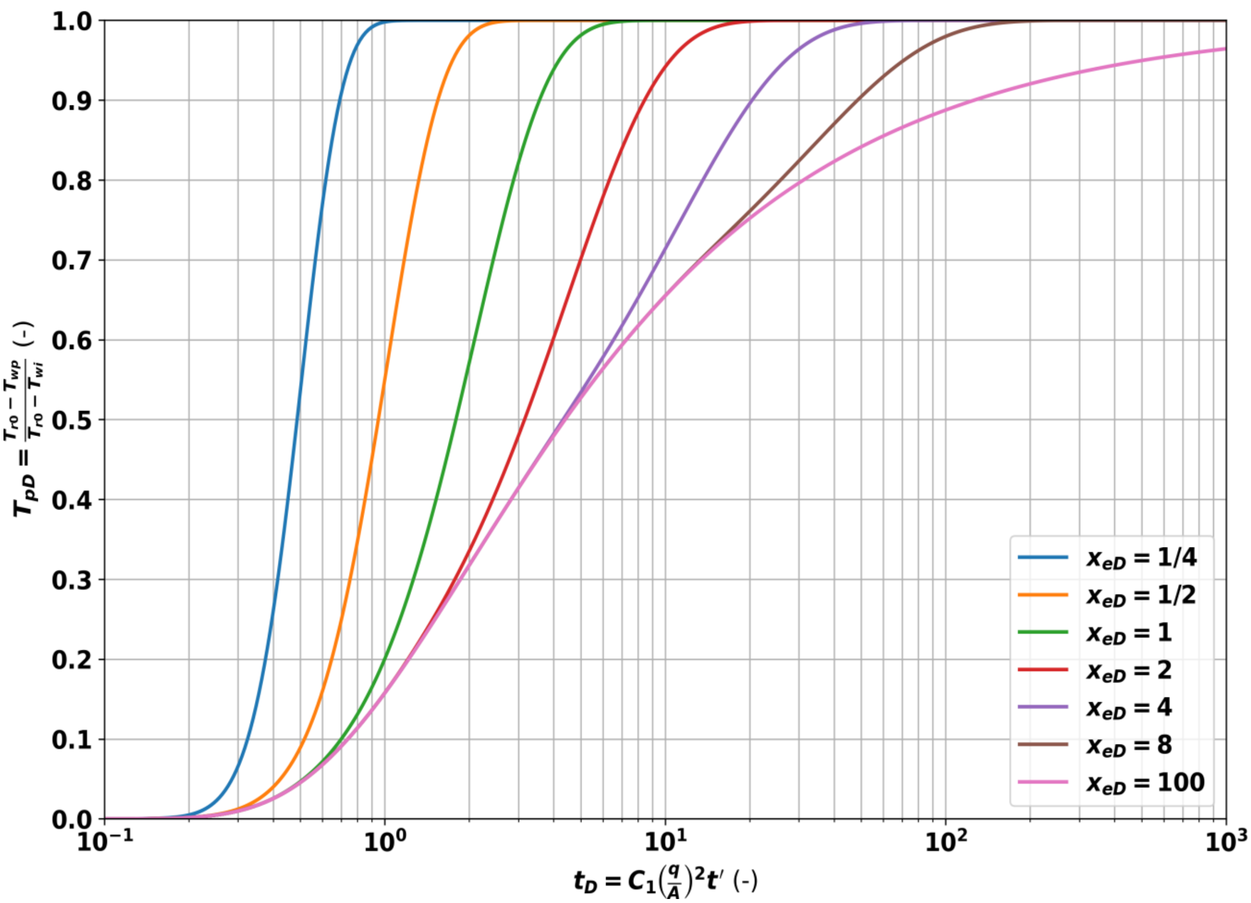

Figure 8: Type curve for production fluid temperature vs. time

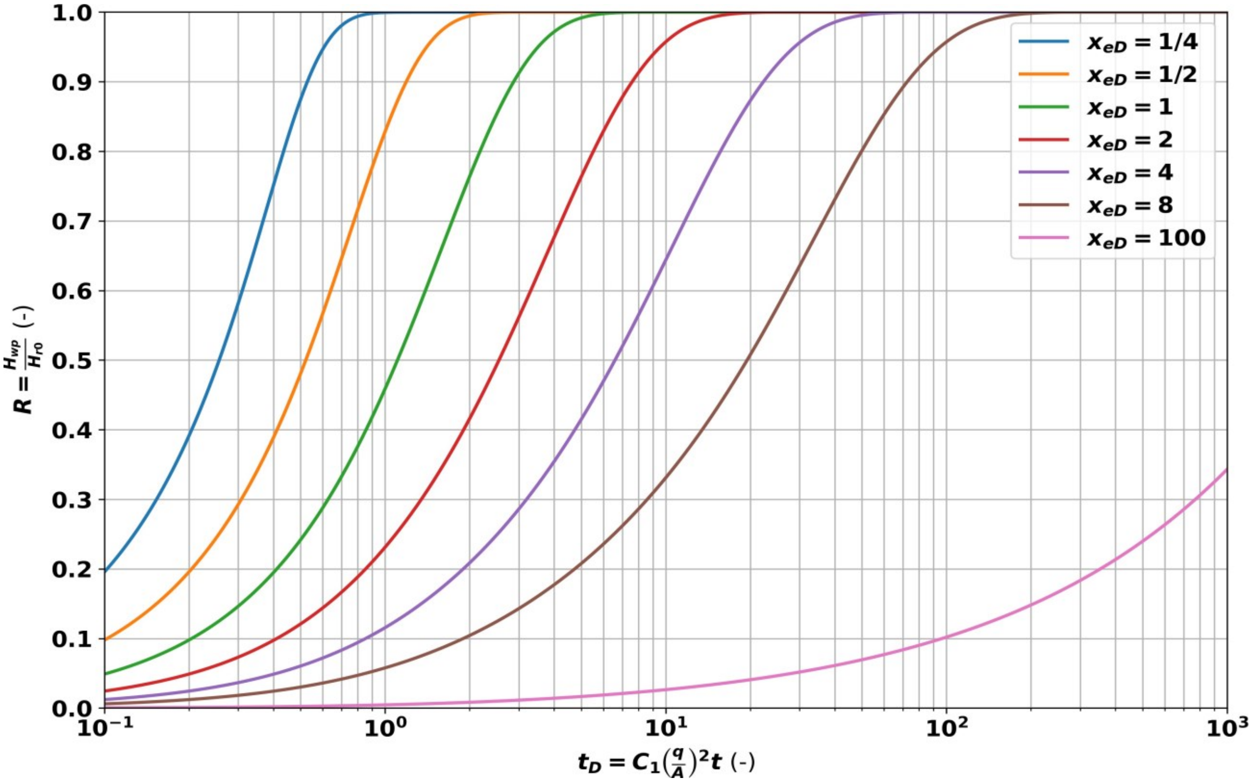

Figure 9: Type curve for thermal recovery factor vs. time

4.2 Example Application for EGS Design Optimization

The type curves and equations for dimensionless temperature (Eq. 6) and dimensionless fracture spacing (Eq. 5) can be used in practical applications for system design, system optimization, and forecasting long-term performance. In Fervo's EGS design, many of the parameters that show up in these equations are either specified as part of the engineering design (e.g., the lateral length and the offset well spacing) or can be well-constrained from multiple independent datasets (e.g., the stimulated reservoir volume (SRV) height, the number of effective flowing fracture pathways, and the effective fracture surface area).

As an example of how to use this type curve theory for EGS design optimization, consider an EGS triplet system that must last for t = 20 years, must produce an initial gross power output of 10 MWe while maintaining a produced fluid temperature that does not drop more than 25 °C below the initial temperature. All other system properties are given below.

The initial gross power output translates to a volumetric flow rate requirement (for each side of the triplet system) of $q = 0.06$ m^3/s. The thermal drawdown constraint translates to a target dimensionless temperature of $T_{wD} = 0.2$. Using Figure 8, the dimensionless time that corresponds to the value of $T_{wD} = 0.2$ ranges from $t_D = 0.65$ for $x_{eD} = 1/2$ to $t_D = 1.3$ for $x_{eD} \geq 2$. For now, assume we take the type curve corresponding to $x_{eD} = 1/2$.

Eq. 6 can be rearranged for the total fracture surface area (Doe et al., 2014; Kennedy et al., 2021):

$$A = q\sqrt{\frac{C_1 t}{t_D}}. \tag{9}$$

This equation can now be used to estimate the total fracture surface area required to meet the system performance requirements:

$$A = 0.06 \text{ m}^3/\text{s} \times \sqrt{\frac{1.41 \times 10^6 \text{ s/m}^2 \times 6.31 \times 10^8 \text{ s}}{0.65}} = 2.72 \times 10^6 \text{ m}^2. \tag{10}$$

This analysis indicates that a total effective fracture surface area of approximately 2.72 km^2 (29.3 million ft^2) would be sufficient to maintain production temperatures above the useful limit for a project duration of 20 years. This can then be used to inform the well design and stimulation treatment design. For example, assuming an effective SRV height of $H = 150$ m and an offset well spacing of $L = 300$ m, the total number of fractures is $N = A/(HL) \approx 50$. Using Eq. 5, the target lateral length can then be determined to be $X_{lat} = 1650$ m.

The thermal recovery factor for this system can also be estimated using the type curves shown in Fig. 2. In this case, we follow the type curve for $x_{eD} = 1/2$ and find where the curve intersects with $t_D = 0.65$. The thermal recovery factor for this EGS design is $R = 0.61$.

From Figure 8, it is clear that for almost all cases of x_{eD}, no thermal decline occurs until $t_D > 0.2$. This observation can be used to determine the time at which point the system is expected to start dropping below the initial production temperature. Rearranging Eq. 6 for t and plugging in our target fracture surface area yields and the value of $t_D = 0.2$ yields $t = 6.2$ years as the point at which the system is expected to begin dropping below the initial production temperature.

5. CONCLUSIONS

Geologic characterization of the Milford Valley has allowed the targeting of a large series horizontal wells across several miles at Fervo's Cape development that have very consistent granitic basement reservoir geometry, allowing standardization of well design and leading to significant reduction of subsurface risk. For a Basin and Range geologic setting, an unprecedented number of deep wells have been drilled in a regular spacing, which provides rarely seen detail in characterizing welded tuff deposits within the basin-fill sediments. A well characterized, stable, conductive temperature regime is nearly flat along the north to south development and has tight temperature controls at both ends, nearly eliminating temperature uncertainty from Fervo's three pad (Frisco-Gold-Bearskin) development at Cape. Linear trends from high-resolution microseismic data collected during hydraulic stimulation of the Frisco wells indicate that the stimulated fractures are dominantly activating the existing NNW-striking natural fracture fabric, rather than aligning to SHmax. Understanding the preexisting fracture networks is important to planning EGS stimulation in hard-rock settings such as the granite at Cape. The application of well-established EGS type curve theory using modern completions engineering design parameters (e.g., lateral length, perforation cluster spacing, stimulated reservoir volume geometry, etc.) can be used effectively to forecast energy production and thermal decline in horizontal well EGS systems.

6. REFERENCES

Brown, D., D. Duchane, G. Heiken, and V. Hriscu, Mining the Earth's Heat: Hot Dry Rock Geothermal Energy, Springer, doi:10.1007/978-3-540-68910-2. (2012).

Cohen, A.: Numerical Methods for Laplace Transform Inversion, Springer (2007).

Dadi, S., Norbeck, J., Titov, A., Dyer, B.: Mohammadi, A., Geng, Y., Obinna, K., and Matson, G., Microseismic Monitoring During a Next Generation Enhanced Geothermal System at Cape Modern, Utah. GRC Transactions, Vol. 48, (2024).

Doe, T., R. McLaren, and W. Dershowitz: Discrete fracture network simulations of Enhanced Geothermal Systems, in 39th Stanford Geothermal Workshop, Stanford, California, USA (2014).

El Sadi, K., Gierke, B., Howard, E., Gradl, C.: Review of Drilling Performance in a Horizontal EGS Development" Proceedings, 48th Workshop on Geothermal Reservoir Engineering, Stanford University, Stanford, CA (2024).

Fercho, S., Norbeck, J., McConville, E., Hinz, N., Wallis, I., Titov, A., Agarwal, S., Dadi, S., Gradl, C., Baca, H., Eddy, E., Lang, C., Voller, K., and Latimer, T.: Geology, state of stress, and heat in place for a horizontal well geothermal development project at Blue Mountain, Nevada, Proceedings, 48th Workshop on Geothermal Reservoir Engineering, Stanford University, Stanford, CA, (2023).

Fercho, S., Matson, G., McConville, E., Rhodes, G., Jordan, R., Norbeck, J.: Geology, Temperature, Geophysics, Stress Orientations, and Natural Fracturing in the Milford Valley, UT Informed by the Drilling Results of the First Horizontal Wells at the Cape Modern Geothermal Project. PROCEEDINGS, 49th Workshop on Geothermal Reservoir Engineering Stanford University, Stanford, California, February 12-14, (2024).

Gringarten, A., P. Witherspoon, and Y. Ohnishi: Theory of Heat Extraction From Fractured Hot Dry Rock, Journal of Geophysical Research, 80 (8), 1120–1124, doi:10.1029/JB080i008p01120, (1975).

Kennedy, B., D. Blankenship, and T. Doe: Performance evaluation of engineered geothermal systems using discrete fracture network simulations: A panel report, Tech. rep., Lawrence Berkeley National Laboratory, doi:10.2172/1775421, (2021).

Kirby, M., Knudsen, R., Kleber, E., Hiscock, A.: Geologic Map of the Utah FORGE Area 1:24,000, Utah Geological Survey - A Division of Utah Department of Natural Resources, (2018).

Norbeck, J., and T. Latimer: Commercial-scale demonstration of a first-of-a-kind Enhanced Geothermal System, EarthArxiv, doi:10.31223/X52X0B, (2023).

Norbeck, J., C. Gradl, and T. Latimer: Deployment of Enhanced Geothermal System technology leads to rapid cost reductions and performance improvements, EarthArxiv, doi:10.31223/X5VH8C, (2024).

Simmons, S.F., Kirby, S., Bartley, R., Allis, A., Kleber, E., Knudsen, T., Miller, J.J., Hardwick, C., Rahilly, K., Fischer, T., Jones, C., and Moore, J.,: Update on the Geoscientific Understanding of the Utah FORGE Site, PROCEEDINGS, 44th Workshop on Geothermal Reservoir Engineering Stanford University, Stanford, California, February 11-13, (2019).